Article

Programming the Internal Structure and Stability of Helical Pores Self-Assembled from Dendritic Dipeptides via the Protective Groups of the Peptide

Virgil Percec, Andrs E. Dulcey, Mihai Peterca, Monica Ilies, Monika J. Sienkowska, and Paul A. Heiney

J. Am. Chem. Soc., **2005**, 127 (50), 17902-17909• DOI: 10.1021/ja056313h • Publication Date (Web): 23 November 2005

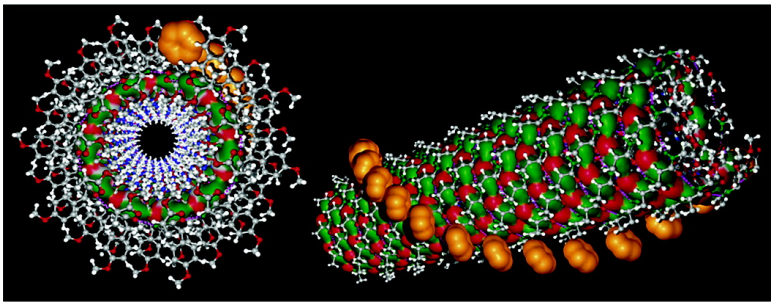

J|A|C|S
ARTICLES
Published on Web 11/23/2005

Programming the Internal Structure and Stability of Helical Pores Self-Assembled from Dendritic Dipeptides via the Protective Groups of the Peptide

Virgil Percec,*,† Andrés E. Dulcey,† Mihai Peterca,‡ Monica Ilies,† Monika J. Sienkowska,† and Paul A. Heiney‡

Contribution from the Roy & Diana Vagelos Laboratories, Department of Chemistry, University of Pennsylvania, Philadelphia, Pennsylvania 19104-6323, and Department of Physics and Astronomy, University of Pennsylvania, Philadelphia, Pennsylvania 19104-6396

Received September 17, 2005; E-mail: percec@sas.upenn.edu

Abstract: The synthesis of dendritic dipeptides (4-3,4-3,5)12G2−CH_2−X−L-Tyr−L-Ala−OMe with X = Boc, Moc, and Ac; their self-assembly in bulk and in solution; and the structural and retrostructural analysis of their supramolecular helical porous assemblies are reported. The dimensions, structure, internal order, thermal stability of the supramolecular helical pores, and conformations of the dendron and supramolecular dendrimer are programmed by the nature of the protective groups of the dipeptide. The ability of the protective groups to program the structure of the helical pore reveals the simplest design strategy that complements the more complex strategies based on the architecture of the dendron, the stereochemistry, and the structure of the dipeptide.

Introduction

Natural pore-forming proteins form the channels that cells use to communicate with one another and the outside world.[1] They also form the coats of viruses,[2] and some have pathogenic[3] and antibiotic[4] activity. Remodeled porous proteins are used in synthetic systems, in the encapsulation of molecules,[5] and in molecular sensing.[6] Synthetic strategies for obtaining porous or tubular supramolecular assemblies have been elaborated.[7] However, with few exceptions,[8] attempts to create synthetic pores capable of assembling into periodically ordered assemblies that are stable both as solids and in solution have yet to be successful. Recently, we reported that amphiphilic dendrons functionalized at their apex with a dipeptide create "dendritic dipeptides" that self-assemble both in solution and in the solid state into supramolecular helical porous structures.[9] This self-assembly process is sufficiently robust to tolerate a range of modifications[9,10] to the structure of the peptide and dendron, and preliminary data showed that these synthetic pores are functional.[9a] Therefore, it is expected that the elucidation of the principles of this self-assembly process will allow the design of a variety of biologically inspired systems with functional properties arising from their porous structure. The structure of the pore is determined by the architecture of the dendron,[9a,10a] the peptide,[9a] and the stereochemistry[9a,10b] of the dipeptide. Here, we report that the protective groups of the dipeptide program both the internal structure and the thermal stability of the helical pores self-assembled from dendritic dipeptides. This unexpected result provides the simplest and one of the most powerful architectural tools available for programming the structure and stability of porous protein mimics self-assembled from dendritic dipeptides.[9]

* To whom correspondence should be addressed.
† Department of Chemistry.
‡ Department of Physics and Astronomy.

(1) (a) MacKinnon, R. *Angew. Chem., Int. Ed.* **2004**, *43*, 4265−4277. (b) Agre, P. *Angew. Chem., Int. Ed.* **2004**, *43*, 4278−4290.
(2) (a) Klug, A. *Angew. Chem., Int. Ed. Engl.* **1983**, *22*, 565−582. (b) Klug, A. *Philos. Trans. R. Soc. London B* **1999**, *354*, 531−535.
(3) Gouaux, E. *J. Struct. Biol.* **1998**, *121*, 110−122.
(4) Wallace, B. A. *Biophys. J.* **1986**, *49*, 295−306.
(5) Ishii, D.; Kinbara, K.; Ishida, Y.; Ishii, N.; Okochi, M.; Yohda, M.; Aida, T. *Nature* **2003**, *423*, 628−632.
(6) Bayley, H.; Cremer, P. S. *Nature* **2001**, *413*, 226−230.
(7) (a) Nolte, R. J. M.; van Beijnen, A. J. M.; Neevel, J. G.; Zwikker, J. W.; Verkley, A. J.; Drenth, W. *Israel J. Chem.* **1984**, *24*, 297−301. (b) Jullien, L.; Lehn, J.-M. *Tetrahedron Lett.* **1988**, 29, 3803−3806. (c) Cross, G. G.; Fyles, T. M.; James, T. D.; Zojaji, M. *Synlett* **1993**, *7*, 449−460. (d) Gokel, G. W.; Ferdani, R.; Liu, J.; Pajewski, R.; Shabany, H.; Uetrecht, P. *Chem. Eur. J.* **2001**, *7*, 33−39. (e) Bong, D. T.; Clark, T. D.; Granja, J. R.; Ghadiri, M. R. *Angew. Chem., Int. Ed.* **2001**, *40*, 988−1011. (f) Sakai, N.; Mareda, J.; Matile, S. *Acc. Chem. Res.* **2005**, *38*, 79−87. (g) Rosselli, S.; Ramminger, A.-D.; Wagner, T.; Silier, B.; Wiegand, S.; Häussler, W.; Lieser, G.; Scheumann, V.; Höger, S. *Angew. Chem., Int. Ed.* **2001**, *40*, 3138−3141. (h) Hill, D. J.; Mio, M. J.; Prince, R. B.; Hughes, T. S.; Moore, J. S. *Chem. Rev.* **2001**, *101*, 3893−4012. (i) Fenniri, H.; Deng, B.-L.; Ribbe, A. E. *J. Am. Chem. Soc.* **2002**, *124*, 11064−11072. (j) Hecht, S.; Khan, A. *Angew. Chem., Int. Ed.* **2003**, *42*, 6021−6024. (k) Couet, J.; Jeyaprakash, J. D.; Samuel, S.; Kopyshev, A.; Santer, S.; Biesalski, M. *Angew. Chem., Int. Ed.* **2005**, *44*, 3297−3301.
(8) (a) Ghadiri, M. R.; Granja, J. R.; Milligan, R. A.; McRee, D. E.; Khazanovich, N. *Nature* **1993**, *366*, 324−327. (b) Petitjean, A.; Cuccia, L. A.; Lehn, J.-M.; Nierengarten, H.; Schmutz, M. *Angew. Chem., Int. Ed.* **2002**, *41*, 1195−1198. (c) Ohkita, M.; Lehn, J.-M.; Baum, G.; Fenske, D. *Chem. Eur. J.* **1999**, *5*, 3471−3481. (d) Schmitt, J.-L.; Stadler, A.-M.; Kyritsakas, N.; Lehn, J.-M. *Helv. Chim. Acta* **2003**, *86*, 1598−1624. (e) Schmitt, J.-L.; Lehn, J.-M. *Helv. Chim. Acta* **2003**, *86*, 3417−3426.
(9) (a) Percec, V.; et al. *Nature* **2004**, *430*, 764−768. (b) Rouhi, M. *Chem. Eng. News* **2004**, *82* (33), 4. (c) Borman, S. *Chem. Eng. News* **2004**, *82* (51), 53−61.
(10) (a) Percec, V.; Dulcey, A. E.; Peterca, M.; Ilies, M.; Miura, Y.; Edlund, U.; Heiney, P. A. *Aust. J. Chem.* **2005**, *58*, 472−482. (b) Percec, V.; Dulcey, A. E.; Peterca, M.; Ilies, M.; Ladislaw, J.; Rosen, B. M.; Edlund, U.; Heiney, P. A. *Angew. Chem., Int. Ed.* **2005**, *44*, 6516−6521.

 10.1021/ja056313h CCC: $30.25

Scheme 1. Synthesis of the Dendritic Dipeptides (4-3,4-3,5)12G2−CH_2−X−L-Tyr−L-Ala−OMe, X = Boc, Moc, Ac

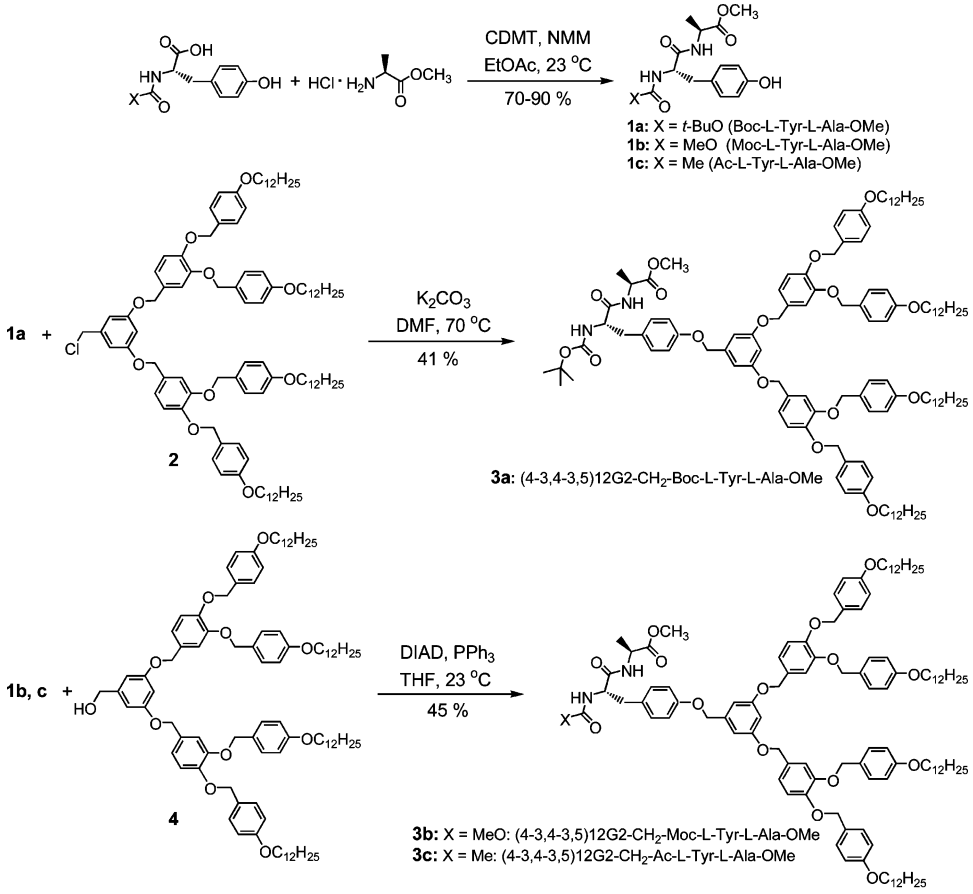

CDMT: 2-Chloro-4,6-dimethoxy-1,3,5-triazene, NMM: *N*-Methyl morpholine, DIAD: Diisopropyl azodicarboxylate

Results and Discussion

Synthesis of Dendritic Dipeptides (4-3,4-3,5)12G2−CH_2−X−L-Tyr−L-Ala−OMe with X = Boc, Moc, and Ac. The dipeptides Boc-L-Tyr−L-Ala−OMe, Moc-L-Tyr−L-Ala−OMe, and Ac-L-Tyr−L-Ala−OMe were synthesized from Boc, Moc, and Ac N-protected L-Tyr with the methyl ester of L-Ala hydrochloride in the presence of 2-chloro-4,6-dimethoxy-1,3,5-triazene (CDMT)[9a,11]/*N*-methyl morpholine (NMM) in EtOAc (Scheme 1) in 70−90% yield after purification by column chromatography (SiO_2/gradient 2−4% MeOH in $CHCl_3$). The dendritic dipeptides were obtained by the Mitsunobu etherification[12] of the hydroxyphenyl group of the dipeptides with (4-3,4-3,5)12G2−CH_2OH.[5,9a,13c] Purities higher than 99% (HPLC) were obtained in 41−45% yield after purification by flash column chromatography (SiO_2/gradient 2−4% MeOH in $CHCl_3$).

Structural and Retrostructural Analysis in the Solid State. A combination of differential scanning calorimetry (DSC) together with small-and wide-angle X-ray diffraction (XRD) experiments recorded during heating and cooling on powder and oriented fibers, electron density maps, simulations of the XRD data, and molecular modeling was used to perform the structural and retrostructural analysis of the supramolecular structures self-assembled from the dendritic dipeptides in the bulk.[9a,13] Phase transitions were determined by DSC, and the structures of the periodic arrays were assigned by XRD. Figure 1 shows the DSC traces of the compounds and summarizes the periodic lattices in which the supramolecular structures self-organize.

All dendritic dipeptides self-assemble into porous supramolecular columns that self-organize into periodic hexagonal columnar arrays. A brief inspection of Figure 1 indicates that three different kind of columns, one with liquidlike intracolumnar disorder (Φ_h), one with short-range intracolumnar helical order, and one with long-range[13e,g] intracolumnar helical order (both labeled Φ_h^{io}), are self-assembled from these dendritic dipeptides. The hexagonal columnar arrays with intracolumnar order differ from conventional hexagonal columnar liquid crystals (Φ_h) that have intracolumnar liquidlike disorder and from 3-dimensional crystals in that no long-range intercolumnar order is available. However, these arrays are expected to be precursors to hexagonal columnar crystals. Examples of intracolumnar order in biological[13f] and synthetic[13g−i] hexagonal columnar assemblies are known. A detailed discussion of these

(11) Kronin, J. S.; Ginah, F. O.; Murray, A. R.; Copp, J. D. *Synth. Commun.* **1996**, *26*, 3491−3494.
(12) Mitsunobu, O. *Synthesis* **1981**, *1*, 1−28.
(13) (a) Percec, V.; Cho, W.-D.; Mosier, P. E.; Ungar, G.; Yeardley, D. J. P. *J. Am. Chem. Soc.* **1998**, *120*, 11061−11070. (b) Percec, V.; Cho, W.-D.; Ungar, G. *J. Am. Chem. Soc.* **2000**, *122*, 10273−10281. (c) Percec, V.; Cho, W.-D.; Ungar, G.; Yeardley, D. J. P. *J. Am. Chem. Soc.* **2001**, *123*, 1302−1315. (d) Percec, V.; Mitchell, C. M.; Cho, W.-D.; Uchida, S.; Glodde, M.; Ungar, G.; Zeng, X.; Liu, Y.; Balagurusamy, V. S. K.; Heiney, P. A. *J. Am. Chem. Soc.* **2004**, *126*, 6078−6094. (e) Zeng, X.; Ungar, G.; Liu, Y.; Percec, V.; Dulcey, A. E.; Hobbs, J. K. *Nature* **2004**, *428*, 157−160. (f) Bernal, D. J.; Fankuchen, I. *Nature* **1937**, *139*, 923−925. (g) Kwon, Y. K.; Chvalun, S. N.; Blackwell, J.; Percec, V.; Heck, J. A. *Macromolecules* **1995**, *28*, 1552−1558. (h) Kwon, Y. K.; Chvalun, S. N.; Schneider, A.-I.; Blackwell, J.; Percec, V.; Heck, J. A. *Macromolecules* **1994**, *27*, 6129−6132. (i) Percec, V.; Rudick, J. G.; Peterca, M.; Wagner, M.; Obata, M.; Mitchell, C. M.; Cho, W.-D.; Balagurusamy, V. S. K.; Heiney, P. A. *J. Am. Chem. Soc.* **2005**, *127*, 15257−15264.

Table 1. Thermal Transitions of (4-3,4-3,5)12G2−CH_2−X−L-Tyr−L-Ala−OMe, X = Boc, Moc, Ac

X	thermal transitions (°C) and corresponding enthalpy changes (kcal/mol)[a] heating	cooling
Boc	$\Phi_{h,g}$[b] 57 Φ_h[c] 96 (5.8) i	i 94 (5.8) Φ_h 53 $\Phi_{h,g}$
Moc	$\Phi_{h,g}^{io}$[e] 55 Φ_h^{io}[d] 80 (−5.2) Φ_h^{io} 109 (1.0) Φ_h^{io} 118 (12.0) i	i 112 (6.4) Φ_h 78 (1.4) Φ_h^{io} 47 $\Phi_{h,g}^{io}$
Ac	$\Phi_{h,g}^{io}$ 57 Φ_h^{io} 120 (0.4) Φ_h^{io} 128 (7.5) i	i 122 (1.7) Φ_h 119 (1.7) Φ_h^{io} 51 $\Phi_{h,g}^{io}$

[a] Thermal transitions (°C) and enthalpy changes (kcal/mol) were determined by DSC (10 °C/min). Data from the second heating and cooling scans are shown. [b] $\Phi_{h,g}$ = glassy state of the hexagonal columnar lattice; [c] Φ_h = *p6mm* hexagonal columnar lattice; [d] Φ_h^{io} = columnar hexagonal lattice with intracolumnar order; [e] $\Phi_{h,g}^{io}$ = glassy state of the hexagonal columnar lattice with intracolumnar order.

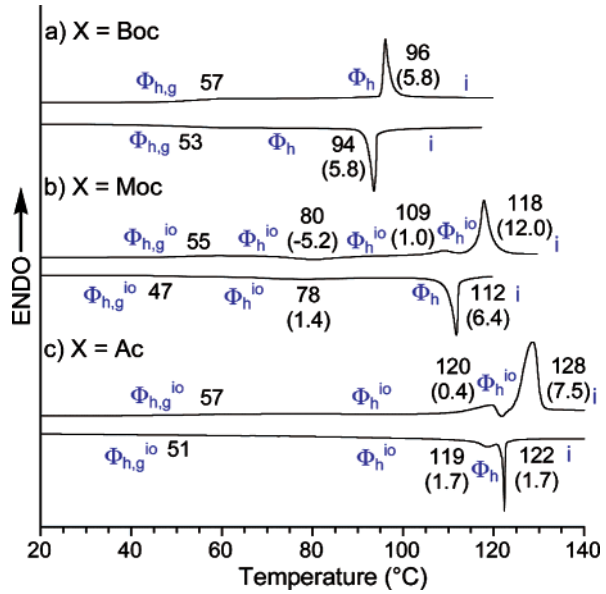

Figure 1. DSC traces (second heating and cooling scans, both at 10 °C/min) of (4-3,4-3,5)12G2−CH_2−X−L-Tyr−L-Ala−OMe: (a) X = Boc, (b) X = Moc, and (c) X = Ac. Transition temperatures are indicated in degrees Celsius, and the corresponding enthalpy changes (in parantheses) are in kilocalories per mole. Φ_h = *p6mm* hexagonal columnar 2-D lattice, Φ_h^{io} = columnar hexagonal lattice with intracolumnar order, $\Phi_{h,g}^{io}$ = glassy state of the hexagonal columnar lattice, $\Phi_{h,g}^{io}$ = glassy state of the hexagonal columnar lattice with intracolumnar order.

intracolumnar ordered structures and their comparison with crystals and liquid crystals will be presented elsewhere. The Boc protective group provides columns that self-organize into hexagonal columnar (Φ_h) lattices. Below the glass transition, their dynamic short-range helical order is frozen, and therefore, this order can be observed by XRD.[9a] The Moc and Ac protective groups mediate self-assembly below 109 and 120 °C, respectively, into supramolecular columns with long-range intracolumnar helical order that self-assemble into hexagonal columnar periodic arrays with intramolecular order (Φ_h^{io}). Above these temperatures, both Moc and Ac form columns with different long-range intracolumnar order (Supporting Information). Upon cooling from the isotropic state, Moc and Ac dendritic dipeptides form a monotropic Φ_h phase similar to that of Boc dendritic dipeptide. In the case of Moc, the Φ_h structure transforms into Φ_h^{io} upon cooling at 78 °C. However, because of the close proximity of this exotherm to the glass transition temperature (T_g), the formation of the Φ_h^{io} phase is completed upon heating above T_g via the exotherm at 80 °C. In the case of Ac, the monotropic Φ_h structure transforms into Φ_h^{io} at 119 °C. In addition to the creation of supramolecular columns with enhanced intracolumnar order, the transition from Boc to Moc and to Ac protective groups increases the stability of the hexagonal columnar lattices by 24 and 32 °C, respectively. All of these results are summarized in Table 1.

Even more remarkable is the effect of the protective group on the intensity of the *d* spacing of the hexagonal columnar lattices self-organized from these supramolecular columns (Figure 2a,b). The porous structure of these columns and their intracolumnar model were demonstrated by a combination of transmission electron microscopy and electron diffraction experiments combined with electron density maps calculated from the XRD data.[9a] D_{pore} is calculated by the simulation of the XRD peak positions and intensities using the electron density of the dendritic dipeptide and considering a three-phase intracolumnar model consisting of aliphatic, aromatic, and peptide regions in addition to the hollow center of the column. Details of this calculation were reported previously.[9a] The application of this method to more complex porous structures will be reported elsewhere. Therefore, the relative intensities of the (10), (11), (20), and (21) *d* spacings provide an immediate indication of the pore diameter (D_{pore}).[9a,10] Previously, we reported that, in the bulk, D_{pore} for Boc-protected dendritic dipeptides is almost constant below the glass transition temperature (T_g) of the supramolecular structure and is strongly dependent on temperature above T_g.[10b] The dependences of the column diameter (D_{col}) and the pore diameter (D_{pore}) on temperature are plotted for all protective groups in Figure 2c,d. The data reported in Figure 2c,d provide two additional important results. The structure of the protective group provides a powerful architectural parameter that programs D_{pore}. This result is not unexpected. However, the fact that Boc provides a larger D_{pore} value than Moc and Ac could not be predicted. In fact, we expected a lower D_{pore} value for the structure self-assembled from the Boc-protected dendritic dipeptide. In addition, in the case of Boc, D_{pore} is stable and temperature-independent below T_g, whereas in the cases of Moc and Ac, D_{pore} is stable for the entire range of temperatures of the Φ_h^{io} phase. This second unpredictable result is very rewarding because it provides a new mechanism to stabilize the porous structure not only in bulk but also in solution. These results are summarized in Table 2. Table 2 also contains the number of dendrons that form the stratum of the supramolecular columns (μ)[9a,13a−d] and the projection of the solid angle (α')[13b,14] of the dendron from the supramolecular column. The role of μ and α' in the ability of the protective groups to program the structure of the pore is discussed later.

Figure 3 shows small- and wide-angle XRD data obtained from the aligned fibers of the dendritic dipeptides. As shown by the X shapes of the *i* and *h* diffractions (Figure 3), all supramolecular columns are helical. However, regardless of temperature, Boc induces a short-range intracolumnar helical

(14) Ungar, G.; Percec, V.; Holerca, M. N.; Johansson, G.; Heck, J. A. *Chem. Eur. J.* **2000**, *6*, 1258−1266.

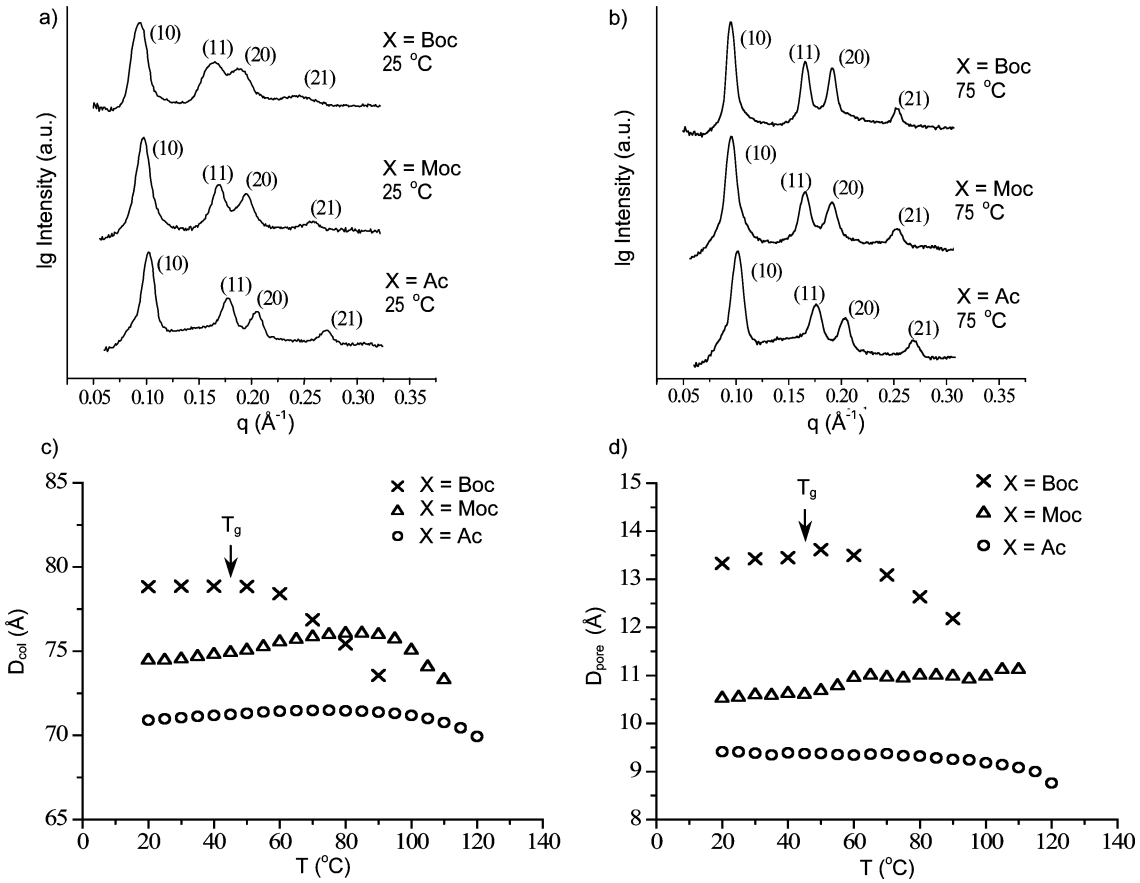

Figure 2. Small-angle X-ray diffraction plots at (a) 25 and (b) 75 °C for the supramolecular structures self-assembled from (4-3,4-3,5)12G2−CH_2−X−L-Tyr−L-Ala−OMe, X = Boc, Moc, Ac. Dependence of the (c) column (D_{col}) and (d) pore (D_{pore}) diameters on temperature.

Table 2. (4-3,4-3,5)12G2−CH_2−X−L-Tyr−L-Ala−OMe Structural and Retrostructural Analysis by XRD

X	*T* (°C)	d_{10}[a] (Å) (A_{10}[b] a.u.)	d_{11}[a] (Å) (A_{11}[b] a.u.)	d_{20}[a] (Å) (A_{20}[b] a.u.)	d_{21}[a] (Å) (A_{21}[b] a.u.)	D_{col} (Å)	D_{pore} (Å)	ρ[c] (g/cm^3)	μ[d] (dendrons/ stratum)	α'[e] (deg)
Boc	20	68.1 (43.5)	39.1 (25.6)	33.9 (24.9)	26.2 (5.9)	78.4 ± 0.4	13.3 ± 1.2	1.02	11.6	31.1
Boc	80	65.6 (44.6)	37.7 (26.0)	32.7 (24.1)	24.7 (5.4)	75.5 ± 0.4	12.6 ± 1.1			
Moc	25	64.4 (55.3)	37.2 (20.9)	32.2 (16.7)	24.4 (7.0)	74.4 ± 0.4	10.5 ± 0.8	1.07	10.6	34.0
Moc	100	65.2 (55.9)	37.5 (20.5)	32.4 (16.5)	24.6 (7.0)	75.0 ± 0.4	10.9 ± 0.8			
Ac	25	61.5 (51.1)	35.4 (24.3)	30.7 (17.2)	23.2 (7.4)	70.9 ± 0.4	9.4 ± 0.7	1.04	9.7	37.2
Ac	100	61.7 (52.1)	35.6 (23.2)	30.8 (17.4)	23.3 (7.2)	71.2 ± 0.4	9.2 ± 0.7			

[a] *d* spacings of the columnar hexagonal phase; [b] Peak amplitude scaled to the sum of the observed diffraction peaks (a.u.=arbitrary units); [c] Experimental density measured at 22 °C; [d] Number of dendrons per column stratum $\mu = (\sqrt{3}N_A D^2 t\rho)/2M$, where $N_A = 6.0220455 \times 10^{23}$ mol^{-1} is Avogadro's number, *M* is the molecular weight of the dendron, and $t = 4.7$ Å is the average height of the column stratum. [e] Projection of the solid angle of $\alpha' = 360/\mu$.

structure, whereas Moc and Ac mediate a long-range[13e,g] intracolumnar helical structure that extends between 16 and 20 layers of column strata. In the case of the supramolecular structure designed from the Moc-based dendritic dipeptide, the calculated radius of the intracolumnar helix is 14 ± 4 Å. The XRD data together with the experimental densities and μ values from Table 2 and molecular modeling experiments were used to construct a molecular model of the supramolecular columns.[9a,10b] The cross sections of the supramolecular pores, without the dendrons, are shown in Figure 4. These structures demonstrate the ability of the protective groups to program the size of the supramolecular pore, their intramolecular order, and the stability of the pore as a function of temperature.

Supramolecular Pore Structure and Stability in Dilute Solution. Previously, we reported that the circular dichroism (CD) and UV spectra of self-assembled dendritic dipeptides in thin films and in dilute solution are similar. Therefore, the supramolecular structures self-assembled from dilute solution and in the solid state are similar.[9a] Self-assembly of dendritic dipeptides occurs in hydrophobic solvents such as cyclohexane, methylcyclohexane, and linear alkanes.[9a,10] The self-assembly in dilute solution can be monitored by a combination of

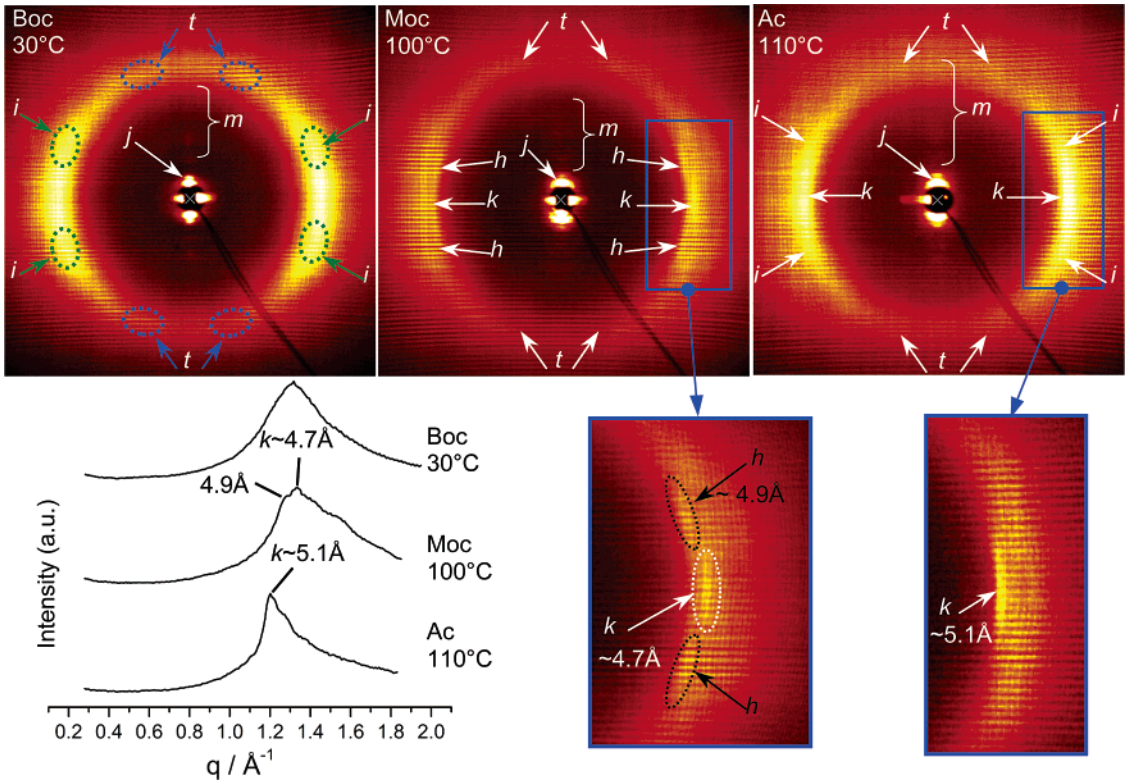

Figure 3. (top) X-ray diffraction patterns collected at different temperatures and (bottom left) wide-angle X-ray diffraction plots for aligned fibers (fiber axis is horizontal) of (4-3,4-3,5)12G2−CH_2−X−L-Tyr−L-Ala−OMe, X = Boc (in Φ_h), Moc (in Φ_h^{io}), Ac (in Φ_h^{io}); *i* = short-range helical feature (~4.5 Å); *t* = tilt feature (64 ± 9°); *j* = (10), (11), and (20) reflections of the Φ_h and Φ_h^{io} phases; *m* = higher-order (*hk*0) reflections; *k* = registry along the column feature (see the insets for representative values; the correlation length is between 16 and 22 layers); *h* = long-range helical feature. The calculated helix radius is 14 ± 4 Å.

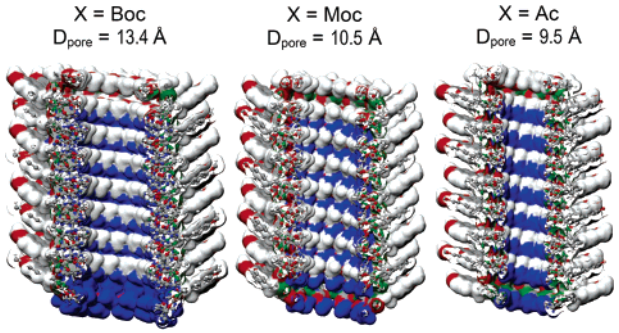

Figure 4. Molecular models of the helical porous columns (cross sections) constructed from XRD and density data and molecular modeling showing the influence of the protective group on the structure of the hydrophobic pores of supramolecular self-assemblies based on (4-3,4-3,5)12G2−CH_2−X−L-Tyr−L-Ala−OMe, X = Boc, Moc, Ac, at 25 °C. Color code: −CH_3 from the protective groups X of Tyr, blue; −CH_3 of the methyl ester of Ala, white; C, gray; O, red; N−H, green. For simplicity, the dendrons are not shown.

spectroscopic methods that include UV spectroscopy, ^{1}H NMR spectroscopy, and CD.[9a] Here, we discuss the self-assembly in solution with the aid of temperature-dependent CD experiments. The CD spectra obtained as a function of temperature during the self-assembly of these dendritic dipeptides are shown in Figure 5. The Cotton effect of the molecular solution of the dendritic dipeptides at high temperature (the right insets in Figure 5) appears at 230 nm. Upon cooling, in all cases, Cotton effects associated with the aromatic part of the dendritic dipeptide are observed.[9a,10] The role of the dipeptide stereochemistry is to select the helix sense of the helical supramolecular structure self-assembled from the dendron.[9a] The stereochemical information of the peptide is communicated to the dendron, and subsequently, a certain dendron conformation mediates the self-assembly of the peptide. However, as demonstrated previously and observed here, any change in the structure of the dipeptide or its protective groups induces changes in the molecular conformation of the dendron and in the supramolecular conformation of the dendrimer.[10b] The reverse of this trend is also valid. This regulation process resembles the allosteric control in proteins.[10b,15] The change of the protective group from Boc to Moc and to Ac induces substantial changes in the CD spectrum of the supramolecular structure. The Cotton effects observed at various wavelengths in Boc-based dendritic dipeptide change both their sign and amplitude in Moc- and Ac-based structures. For the purpose of the present discussion, it is important to notice that the ellipticity of the maximum Cotton effect of the CD spectra increases at the transition from Boc to Moc and Ac. This trend is in line with the short-range versus long-range intramolecular helical structure observed in bulk experiments (Figure 5). Additional important information obtained from these experiments refers to the melting temperature (T_m) of the individual supramolecular columns that is obtained from the plot of ellipticity versus temperature (lower insets in Figure 5).

The transition from Boc to Moc and to Ac also increases T_m from 22 to 38.5 and 47.5 °C, respectively (Figure 5, lower right insets). This result correlates with the trend of the transition temperatures obtained in the solid state (Figure 1, Table 1) and is extremely important because it demonstrates that the protective groups of the dipeptide provide a mechanism for enhancing

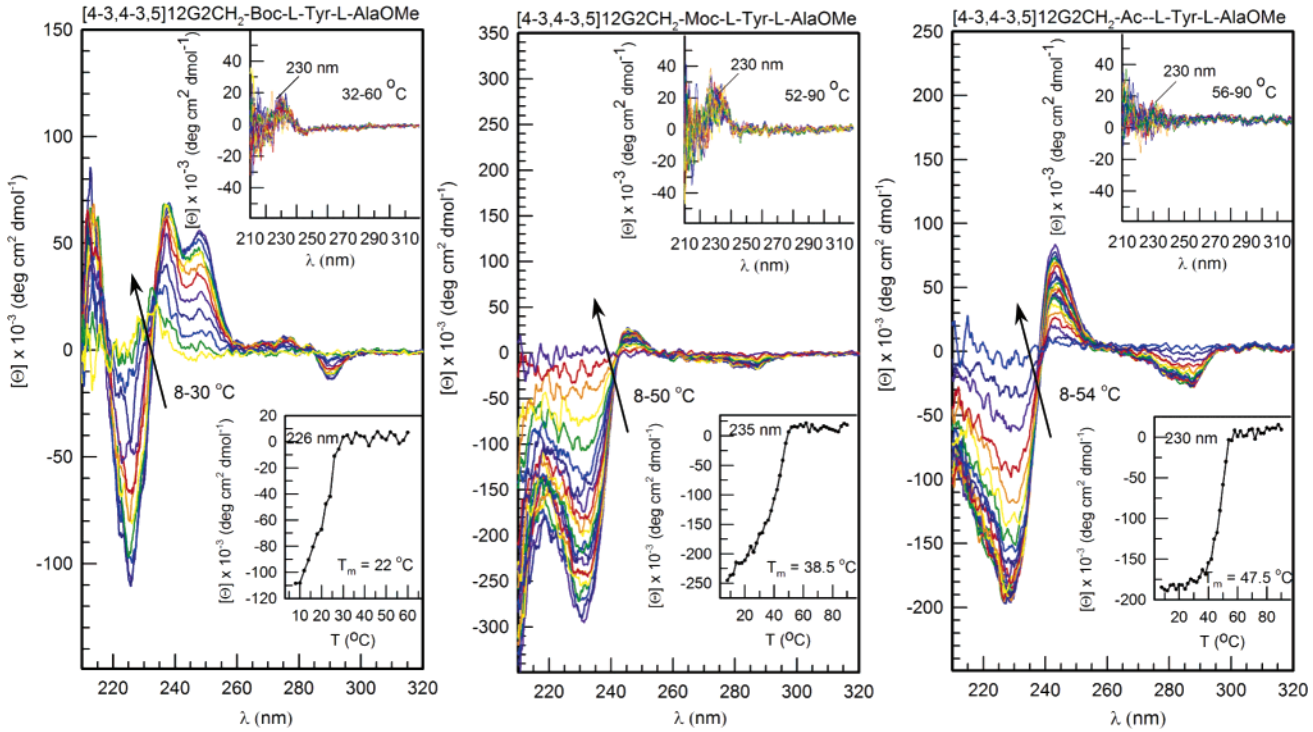

Figure 5. CD spectra of (4-3,4-3,5)12G2−CH_2−Boc-L-Tyr−L-Ala−OMe (1.6×10^{-4} M in cyclohexane) and (4-3,4-3,5)12G2−CH_2−X−L-Tyr−L-Ala−OMe, X = Moc, Ac (1.1×10^{-4} M in methylcyclohexane/cyclohexane 3/1 v/v). Arrows indicate trends upon increasing temperature. The upper insets illustrate the Cotton effect associated with the molecular solution of the dendritic dipeptide. The bottom insets show the molecular ellipticity as a function of temperature at the wavelength at which the intensity of the Cotton effect is maximum. The melting temperatures (T_m) determined from these plots are also indicated.

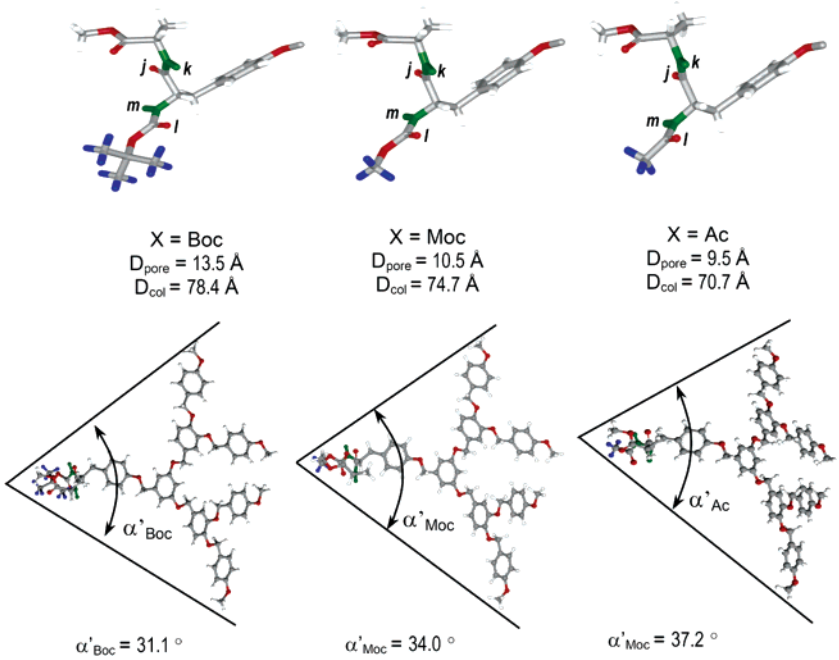

Figure 6. (top) Conformations of (4-3,4-3,5)12G2−CH_2−X−L-Tyr−L-Ala−OMe, X = Boc, Moc, Ac, in their supramolecular structures from Figure 4 (only the first methyl ether of the dendron is shown). (bottom) Correlation between the protective group of the dipeptide and the pore (D_{pore}) and column (D_{col}) diameters self-assembled from dendritic dipeptides. The structure of the protective group changes the projection of the solid angle (α'_X) of the dendritic dipeptide and results in different D_{pore} and D_{col} values. Color code: $-CH_3$ from the protective group of Tyr, blue; $-CH_3$ of the methyl ester of Ala, white; C, gray; O, red; N−H, green. The atoms that generate the in-layer H-bonds of the supramolecular columnar assembly are labeled *j*−*k* and *l*−*m* (see Figures 7 and 8 for details).

the thermal stability of the single pore required for single-channel transport experiments carried out in artificial membranes.[9]

Mechanism of Pore Programming by the Protective Groups of the Dipeptide. The cooperative transfer of structural and stereochemical information between the dendron and the dipeptide is responsible for the mechanism by which the structure and stability of the pore are programmed. Figure 6 shows the conformation of the dipeptides as they exist in the dendritic dipeptides forming the pore structures shown in Figure

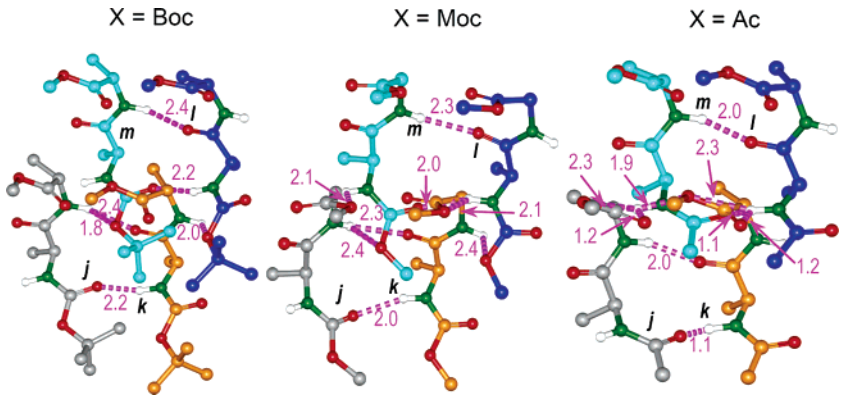

Figure 7. H-bonding network (lengths in angstroms) of the supramolecular pore structures from Figure 4 of (4-3,4-3,5)12G2−CH_2−X−L-Tyr−L-Ala−OMe, X = Boc, Moc, Ac, at 25 °C. Four dipeptides from two layers are illustrated: In the top layer, the two dipeptides are shown with C atoms in light blue and dark blue; in the bottom layer, one of the two dipeptides has the C atoms in gray, and the other one has them in gold; O, red; N, green; phenyl of Tyr and H atoms are not shown except the N-bound H, which is shown in white. The column axis is vertical, and the in-layer directional H-bonds are labeled *l*−*m* and *j*−*k*.

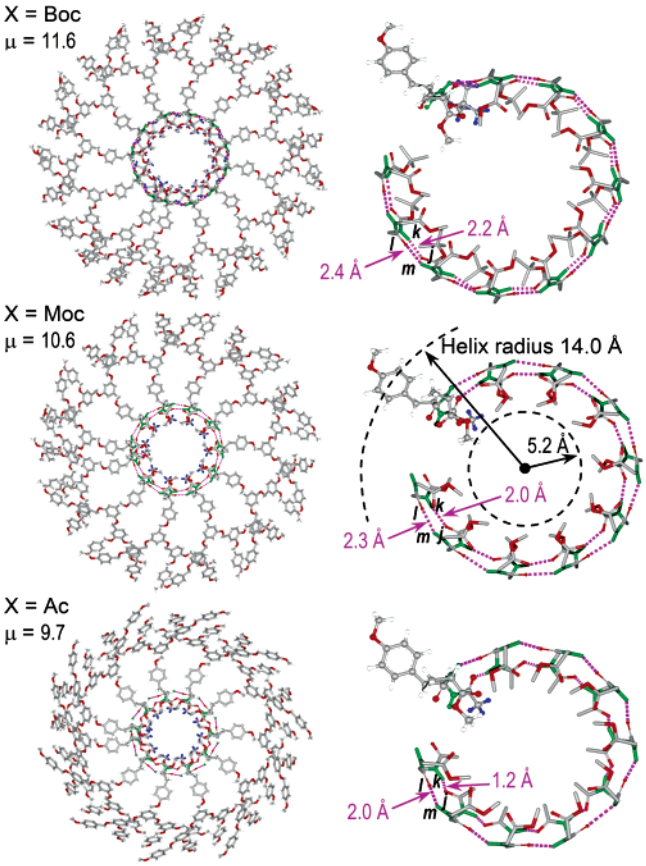

Figure 8. (left) Top views of one layer of the columns whose cross sections are shown in Figure 4 and (right) detail of the H-bonding for (4-3,4-3,5)-12G2−CH_2−X−L-Tyr−L-Ala−OMe, X = Boc, Moc, Ac, at 25 °C. The first two H-bonds seen when viewing Figure 7 from its top (*m*−*l* and *j*−*k*) are shown on the right side. The long-range helical feature calculated from fiber XRD and indicated by *h* in Figure 3 is shown in the middle right side for Moc. Color code: −CH_3 from the protective groups X of Tyr, blue; −CH_3 of the methyl ester of Ala, white; C, gray; O, red; N−H, green. The in-layer directional H-bonds are labeled *j*−*k* and *l*−*m* (see Figures 6 and 7 for details). For simplicity, only the first methyl ether of the dendron is shown in each case.

4. The projections of the dendritic dipeptide conformations, together with the values of the projections of their solid angles (α′)[14] from Table 2, are shown in Figure 6. An increase in α′ from Boc- to Moc- and to Ac-based dendritic dipeptides is accompanied by a decrease in the number of dendrons required to create a column stratum (μ). The change in μ will affect the H-bond length and strength in the dipeptide network and, therefore, will determine the stability of the pore (Figures 7 and 8).

As shown previously,[9a] the self-assembly of the dendron induces a parallel arrangement of the dipeptide in the helical porous structure. This arrangement mediates the construction of a supramolecular network of H-bonds. This helical and parallel arrangement of H-bonded peptides is not known in biological and native artificial proteins and peptides that prefer an antiparallel arrangement during H-bonding. Figure 7 illustrates the impact of the protective groups in this H-bonded network. The transition from Boc to Moc and to Ac induces the shortening of the H-bond distances and consequently increases the stability of the porous structures both in the solid state (Figure 1) and in solution (Figure 5). This mechanism programs the stability of the internal structure of the pore. The number of dendrons (μ) forming the cross section or the stratum of the porous column (Table 2) determines the size of the pore (Figure 4), as shown in the schematic representation in Figure 8. Moc and Ac protective groups mediate the self-assembly of a higher intracolumnar order, which provides an enhanced supramolecular polymer effect[10a,16] through H-bonding. This supramolecular polymer effect explains the increase in the stability of the supramolecular columns both in the solid state and in solution via the same thermodynamic schemes elaborated for the covalent polymer effect.[16] It is extremely rewarding to see the remarkable power of the protective groups and their ability to provide the simplest architectural motif for the design and construction of porous structures from dendritic dipeptides.

Previous approaches to control μ, α′, D_{pore}, and pore stability were accessible through different chemical structures of the self-assembling dendron attached to the dipeptide,[10a] the dipeptide stereochemistry,[9b] and the dipeptide structure.[9a]

(15) (a) Monod, J.; Changeux, J.-P.; Jacob, F. *J. Mol. Biol.* **1963**, *6*, 306−329. (b) Perutz, M. *Mechanism of Cooperativity and Allosteric Regulation in Proteins*; Cambridge University Press: Cambridge, U.K., 1990. (c) Evans, P. R. *Curr. Opin. Struct. Biol.* **1991**, *1*, 773−779.
(16) (a) Percec, V.; Keller, A. *Macromolecules* **1990**, *23*, 4347−4350. (b) Percec, V.; Ahn, C.-H.; Ungar, G.; Yeardley, D. J. P.; Möller, M.; Sheiko, S. S. *Nature* **1998**, *391*, 161−164. (c) Percec, V.; et al. *J. Am. Chem. Soc.* **1998**, *120*, 8619−8631.

Conclusions

Self-assembling dendritic dipeptides provide a general strategy for the design of supramolecular helical porous protein mimics and of their function.[9,10] Therefore, elucidation of the role of each molecular component of the dendritic dipeptide in the self-assembly process is required. Previously, we reported preliminary data that provided fundamental design principles with strategies based on dendron architecture and dipeptide structure and stereochemistry. In this article, we demonstrated the capability of the protective groups of the dipeptide to program the dimensions, structure, internal order, thermal stability, and conformation of the dendron and of the supramolecular dendrimer in the supramolecular helical pores. This concept provides the simplest architectural motif that expands dramatically the scope and limitations of self-assembling dendritic dipeptides in the construction of supramolecular structures programmed on all structural levels.[17]

Acknowledgment. Financial support from the National Science Foundation (DMR-0548559) and Office of Naval Research and discussions with Professor G. Ungar of U. Sheffield, U.K., are gratefully acknowledged.

Supporting Information Available: Experimental section, materials, techniques, and synthesis with structural analysis results. This material is available free of charge via the Internet at http://pubs.acs.org.

JA056313H

(17) Rowan, A. E.; Nolte, R. J. M. *Angew. Chem., Int. Ed.* **1998**, *37*, 63−68. (b) Hirschberg, J. H. K. K.; Brunsveld, L.; Ramzi, A.; Vekemans, J. A. J. M.; Sijbesma, R. P.; Meijer, E. W. *Nature* **2000**, *407*, 167−170. (c) Green, M. M.; Park, J.-W.; Sato, T.; Teramoto, A.; Lifson, S.; Selinger, R. L. B.; Selinger, J. V. *Angew. Chem., Int. Ed.* **1999**, *38*, 3139−3154. (d) Hecht, S. *Mater. Today* **2005**, *8*, 48−55. (e) Emrick, T.; Frechet, J. M. J. *Curr. Opin. Colloid Interface Sci.* **1999**, *4*, 15−23.